1st Croatian Conference on Earthquake Engineering
1CroCEE
22-24 March 2021 Zagreb, Croatia

DOI: https://doi.org/10.5592/CO/1CroCEE.2021.178

Probabilistic Seismic Assessment of existing RC framed structures under earthquake sequences and exposed to pitting corrosion

Francesco Pugliese[1], Luigi Di Sarno[2]

[1] *PhD Candidate in Seismic Analysis and Risk Assessment*, School of Engineering and Institute for Risk and Uncertainty, University of Liverpool, Liverpool, United Kingdom, *francesco.pugliese@liverpool.ac.uk*

[2] *Senior Lecturer in Structural and Earthquake Engineering*, School of Engineering and Institute for Risk and Uncertainty, University of Liverpool, Liverpool, United Kingdom, *luidi.di-sarno@liverpool.ac.uk*

Abstract

Earthquake swarms are catastrophic events that affect the global strength, stiffness and ductility of existing reinforced concrete (RC) structures due to the effects of damage accumulation. Such multiple excitations can be more critical if RC buildings are exposed to highly aggressive environments. In this study, the seismic performance of a four-story RC framed structure exposed to corrosion and subjected to multiple earthquakes is assessed and compared in terms of fragility. A finite element model for the RC frame is adopted and implemented in an advanced software platform for seismic simulations. To provide a complete prediction and understanding of structural response uncertainties, the geometrical and the mechanical properties of steel and concrete constitutive models are defined independent random variables with specific probabilistic distributions. The long-term exposure to aggressive environments is simulated through the pitting corrosion with its probabilistic time initiation and propagation. Such pitting corrosion is applied to beams and columns.

Montecarlo simulations are then performed to investigate the seismic performance of the testbed RC frame through Incremental Dynamic Analyses (IDA). The chord rotation and shear forces of RC components, accounting for brittle and ductile mechanisms, are used as engineering demand and capacity parameters. The robust fragility assessment is then conducted for a range of seismic intensity, i.e., (a) the spectral acceleration for the first fundamental frequency of the structure and (b) the modified spectral acceleration intensity accounting for the elongation period. Finally, the fragility assessment of environmental marine exposure is presented and compared to the pristine structure.

Key words: corrosion, RC structures, earthquake engineering, numerical modelling, probabilistic assessment, fragility analysis

1 Introduction

Over the last decades, many RC structures have experienced multiple aftershocks after a main earthquake event [1]. Such multiple excitations are extremely detrimental phenomena that may affect significantly the seismic resistance of existing RC buildings, namely due to the short time of occurrence between mainshocks and aftershocks [3-5]. It is recognized that old RC structures were designed to withstand single strong motions and with poor seismic details (i.e., bar lap length, stirrups spacing, diameter of transverse reinforcement, low compressive strength for concrete). In addition, a significant percentage of such ordinary buildings is facing severe serviceability and durability conditions due to highly-corrosive environments [2]. Potentially, the environmental deterioration attack coupled with strong multiple ground motions could have large negative effects on the mechanical and geometrical properties of RC components which may cause extensive damage and structural collapse [6, 7]. Yet, the environmental exposure over the lifetime of RC structures necessitates the time-dependent fragility assessment to account for the corrosion initiation and propagation, alongside a probabilistic approach to include the uncertainty in the model parameters and deterioration variables. This study investigates the seismic vulnerability of a typical RC frame, built in Italy between the 60s and 70s, exposed to corrosion and subjected to earthquake sequences. Firstly, fifteen mainshocks and aftershock are collected from international databases. Mainshocks and aftershocks are merged with a time gap equal to ten times the first natural period of the structure to simulate multiple excitations and cease any move due to damping. Then, the description of the finite element (FE) model of the RC frame is presented. The FE model is implemented in an advance software platform for earthquake engineering analyses (Opensees, https://opensees.berkeley.edu/). An introduction to the probabilistic modelling approach for the pitting corrosion and the seismic fragility assessment is provided. Finally, the fragility curves are built based on the probabilistic approach of the IDA by using the limit state of near collapse and two seismic intensity measure (IM) (i.e., (a) the spectral acceleration at the first natural period of the un-corroded and corroded structure ($Sa[T_1]$), and (b) the modified acceleration spectrum intensity (MASI) between the first natural period and the elongated period from the time history analysis)

2 Ground motions selection and limit states definition

Within the framework of seismic risk assessment, the selection of ground motions is a crucial task to provide reliable and accurate inelastic responses of RC framed structures. Despite the selection of earthquake signals is based on the soil specification, structure location and target response spectrum, a set of fifteen as-recorded ground motions (mainshocks and aftershocks) were collected from international database to simulate real earthquake swarms. The latter allows a proper identification of the structural response in comparison with the use of either artificial or scaled records.

Furthermore, the choice of an adequate seismic IM, which complies with recognized feasible criteria for optimal parameters (i.e., efficiency, proficiency, sufficiency and practicality), is essential for the vulnerability assessment of RC structures over their lifetime [10]. As a result, the 5 % damped spectral acceleration at the first natural period ($Sa[T_1]$) and the modified acceleration spectral intensity (MASI) are adopted for the fragility analysis. The limit state of near collapse was considered for the structural performance assessment of the testbed RC frame. Such a limit state complies with Eurocode 8 [11]. According to such selection, the flexural capacity and shear capacity were examined. Such structural behaviours were included to account for ductile mechanisms (by means of the chord rotation) and brittle mechanisms (by means of shear strength). It is assumed that the formulations by [11] still apply when corrosion occurs; while, the yielding and the ultimate curvature, as well as the mechanical properties of RC cross-section are computed according to the level of the corrosion rate. The demand-capacity ratio is taken as structural performance for the examined limit state and denoted as Y_{LS} (Y_{LSb} for brittle mechanisms Y_{LSd} for ductile mechanisms).

$$YLS_{b,d} = max_{i=1}^{N_{ele}} \left[\left(\frac{D_i}{C_i} \right)_b , \left(\frac{D_i}{C_i} \right)_d \right] \tag{1}$$

3 Chloride Corrosion Modelling

High chloride contents on steel reinforcement is one of the most critical factors for the reduced performance of RC structures exposed to harsh environments. The chloride-induced corrosion process can be divided into three subcategories that include: corrosion initiation, propagation and deterioration.

3.1 Corrosion initiation

The most adopted and recognized model for the time initiation [12] is based on the diffusion process defined by Fick 'second law. Such a probabilistic model assumes that the initial value of the chloride content inside the concrete is zero, while the initiation of corrosion occurs when the chloride concentration on the steel bars reaches a critical value. The time initiation can be expressed as:

$$t_{init} = X_1 \left\{ \frac{cover\_depth^2}{4 k_e k_c k_t D_0 t_0^{\alpha}} \left[erf^{-1} \left(1 - \frac{C_{cr}}{C_0} \right) \right]^{-2} \right\}^{\frac{1}{1-\alpha}} \tag{2}$$

Further details on statistical distributions of the model parameters in eq. (2) can be found in [12]. Moreover, depending on the type of exposure (i.e., (a) submerged, (b) tidal, (c) splash and (d) atmospheric), such model parameters tend to change. Performing a

Montecarlo simulation over 100000 samples (Fig. 1a), the predicted time initiation of corrosion can be estimated by a lognormal statistical distribution (Fig 1a-1b). The lognormal distribution refers herein to the splash exposure.

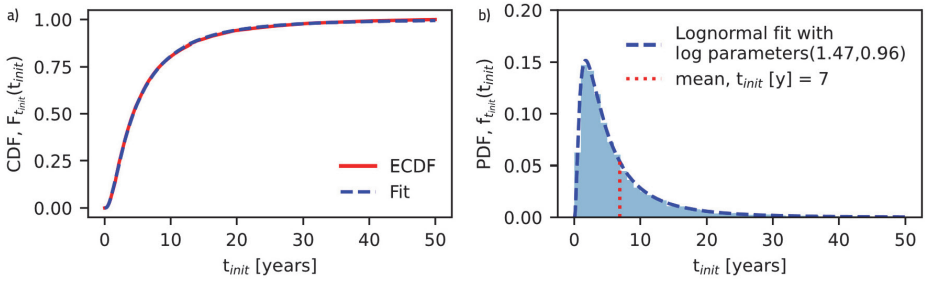

Figure 1. a) Numerical Evaluation (ECDF vs Fitting) of the time initiation, b) Lognormal PDF fitting distribution for time initiation

3.2 Corrosion Propagation and deterioration

Once corrosion initiates, the chloride ingress leads to a de-passivation of the protective film surrounding the steel reinforcement. As a result, the velocity of corrosion rate becomes the key factor in the deterioration of steel rebars. Although harsh environments may lead to (a) uniform or (b) pitting corrosion, several investigations have indicated that localized corrosion (b) is most likely to occur in RC elements [2]. The end of corrosion propagation phase coincides with the onset of the cracking initiation (time for crack initiation, t_{cr}), which can be expressed by:

$$p(t) = R\int_{t_{init}}^{t_{cr}} r_i(t)\,dt \tag{3}$$

When the pitting depth p(t) reaches the critical penetration ($p_{crit}(t)$), the concrete cover begins to crack. The experimental results of [13] were taken herein to determine whether or not the data followed a specific probabilistic distribution for the cover cracking initiation. More specifically, it is assumed that the variance of residuals of the regression model is homoscedastic (constant variance), while a lognormal regression is used to interpolate the data. Figure 2a shows that the outcomes of such a regression model well fit the experimental results. Therefore, the critical crack penetration can be defined by a lognormal distribution with mean computed through the equation in Figure 2a and a constant standard deviation equal to 0.18.

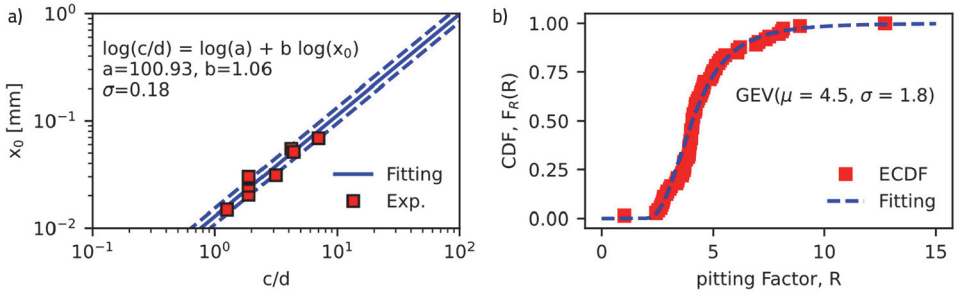

Figure 2. a) Regression model for the critical crack initiation, b) Pitting Factor statistical distribution (*keynote*: GEV – Generalized Extreme Value)

The pitting factor R, likewise, is paramount for the assessment of RC structures as its use is intend to define the critical pit depth and influence the residual capacity of reinforcing bars. Some experimental studies were carried in the literature to study the realistic range of such a factor, but only few focussed on diameters of interest in the framework assessment of typical RC components ([14-16]). Thus, only the experimental campaigns with longitudinal steel bar diameters (12mm, 13mm and 16mm) complying with existing RC structures were collected to identify the statistical distribution of the pitting factor. The generalized extreme value seems (Figure 2b) to accurately and reliably fit the values of R obtained from short- and long-term experimental studies. Using the equation for the critical pitting depth in Fig. 2a and the factor R from the statistical distribution, the formulation (3) can be solved for the time-to-cracking initiation, which represents the mean of a lognormal distribution. The standard deviation instead was computed from the results given by [19], by performing a Montecarlo simulation over 50000 samples. Thus, the time-to-cracking could be described by a lognormal distribution with the coefficient of variation equal to 0.53, which is used in this study.

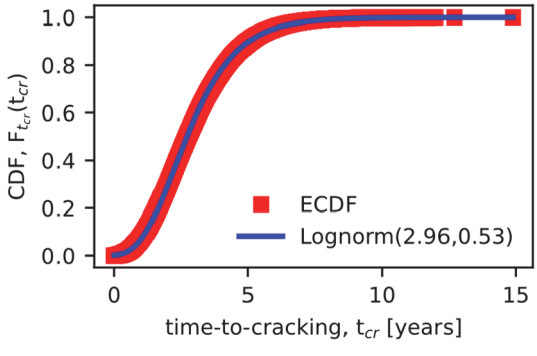

Figure 3. Numerical fitting of time-to-cracking

After cracking initiation and degradation of the protective passive film layer around the steel bars, corrosion leads to two specific phases, such as severe cracking and spalling

of the concrete cover. The severe cracking is typically associated with a crack width equal to 0.3mm (Eurocode 2), while the spalling of the concrete cover is 1mm according to [17]. The reduction of the steel rebar area due to pitting corrosion can be calculated using the model proposed by [18]:

$$w(t) = 0.0575\left[A_i - A_{i+1}\right] \tag{4}$$

Once the value of A_{i+1} is obtained from eq. (4), it is then possible to compute the pit depth at either cover severe cracking or cover spalling, solving the following formulation for t_{i+1}:

$$p_{i+1}(t) = p_{i+1}(t) + R\int_{t_{init}}^{t_{cr}} r_i(t)\,dt \tag{5}$$

4 Case study analysis

4.1 RC Frame description

An existing 4-storey RC frame was used as testbed in this study. Such a frame represents a typical configuration used in Italy between the 60 s and 70 s. The RC columns had a cross-section of 350 x 350 mm^2 at the ground floor and 300x300 mm^2 for the remaining floors, reinforced with 6φ16 longitudinal rebars and ϕ6 transversal stirrups with 200 mm spacing. The beams had cross-sections of 300x500 mm^2 at the first and the fourth floor, reinforced with 8φ14 longitudinal rebars, and 800x200 mm^2 at the second and third floors with 12φ14 longitudinal bars. All the beams had φ6 transversal stirrups with 150 mm spacing.

Table 1. Mechanical properties of the materials

Parameter	**Mean** [MPa]	COV	Probabilistic Distribution type
f_c	16.73	0.10	Lognormal
f_y	440	0.10	Lognormal
E_s	200000	0,20	Lognormal
cover	30	0.15	Normal

The compressive strength of concrete and the yielding stress of steel reinforcement were set at 20 MPa and 440 MPa according to original specifications, while a confidential factor of 1.2 was applied for the uncertainties related to the material properties (Table 1). The distributed plasticity through force-based elements with five integrations point was adopted for beams and columns. Each of integration points includes the RC cross-section discretized into small fibres with a specific mesh density (200 fibres) and stress-strain relationship. The Kent-Park Concrete01 and Giuffre-Menegotto Steel02 in Opensees were used to simulate the constitutive models for the concrete and the steel

reinforcement and modified according to the corrosion rate. Moreover, the zero-length section element was implemented at the base of the structure for the strain penetration and bar slipping. The models of concrete and steel reinforcement in the zero-length were used as Force-displacement: the concrete strains were multiplied by 5 times the diameter of the mean steel bar, while the model of Zhang was adopted for the steel reinforcement. The FE model of the RC frame is shown in Figure 3.

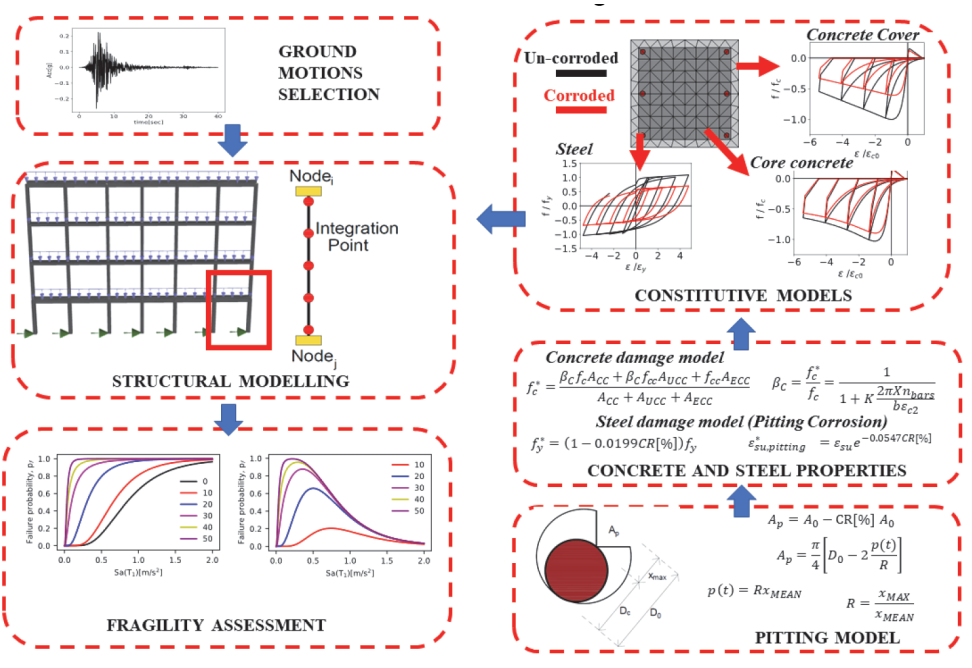

Figure 4. Model Layout

5 Seismic fragility assessment

The seismic fragility assessment is the conditional probability of a specific intensity measure at a given limit state, which represents the occurrence of the seismic demand exceeding the structural capacity. The fragility curves can be expressed as the cumulative density function for a given IM that reaches the limit state threshold. Such fragility curves are obtained by performing nonlinear dynamic analyses IDA-based. This technique involves scaled-ground motions until the onset of the specified limit is reached.

$$P(IM^{YLS=1} < IM) = \phi\left(\frac{\ln IM - \ln \eta_{IM}^{YLS=1}}{\beta_{IM}^{YLS=1}}\right) \tag{6}$$

$$\ln\eta_{IM}^{YLS=1} = \frac{1}{n}\sum_{i=1}^{n_{records}} IM_i^{YLS=1}, \sigma_{\ln\eta_{YLS|IM}} = \sqrt{\frac{\sum_{i=1}^{n}\left(\ln YLS_i - \ln\eta_{YLS|IM}\right)^2}{n-1}} \quad (7)$$

where $\eta_{IM}^{YLS=1}$ and $\beta_{IM}^{YLS=1}$ are the mean and the standard deviation of the intensity measure at the onset of the limit state.

5.1 Fragility curves IDA-based

The outcomes from the numerical simulations of the case-study RC frame exposed to corrosion and subjected to single and multiple earthquakes are shown in Figures 4 and Figures 5. Such results show how the probability of exceeding the limit state of near collapse increases over the lifetime of the RC frame due to the non-uniform chloride attacks. The effects of pitting corrosion, in fact, may lead to a strong deterioration and extensive damage, which is different if RC structures are subjected to single or multiple earthquake excitations. Although the RC frame exhibits an increase in the failure probability for all earthquake conditions, multiple excitations have a higher impact on the seismic vulnerability compared to mainshock and aftershock motions. For instance, the increase in the failure probability for the sequential motions is equal to 43 % at time of 10 years in comparison with 25 % for mainshocks and 19 % for aftershocks for the IM of the spectral acceleration.

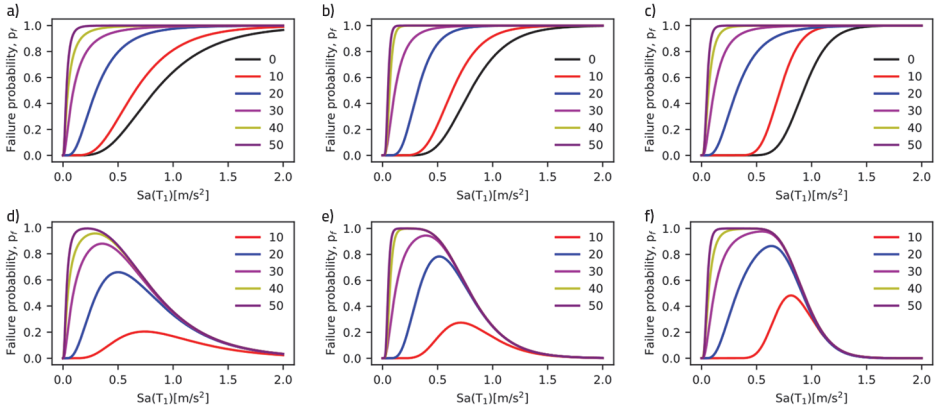

Figure 5. Fragility Curves and fragility difference: (a-d) Aftershocks, (b-e) Mainshocks and (c-f) Sequences

The mean values of the fragility curve that would cause collapse of the RC frame with a probability of 50 % decreases over time. For instance, such a value was reduced by 65 % (Sa(T_1) = 0.32g) at time of 20 years for earthquake sequences, while 60 % for mainshocks and aftershocks. It is also worth noticing that the fragility curves move closer with the increase of time; this is because the corrosion rate decreases and results in

smaller deterioration effects on the RC frame. For example, the fragility curves at time 40 and 50 years are closer than the curves for 10 years and 20 years, regardless of the IM used for the fragility assessment.

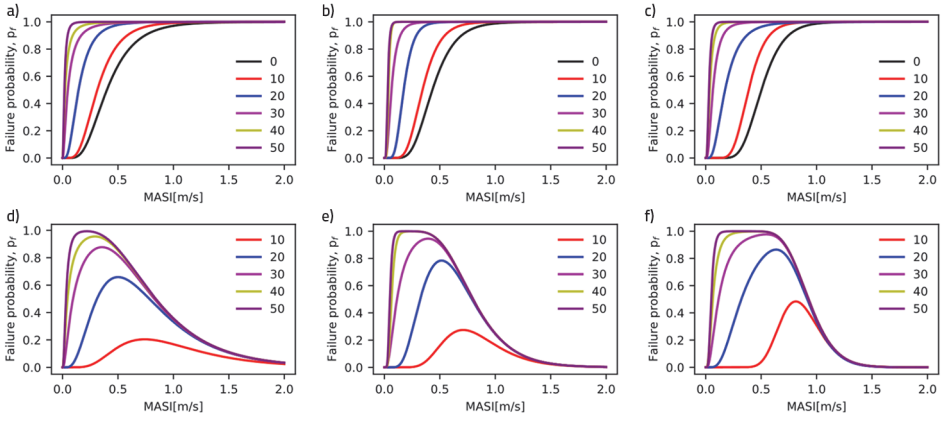

Figure 6. (Fragility Curves and fragility difference: (a-d) Aftershocks, (b-e) Mainshocks and (c-f) Sequences

RC structures with a long-term exposure to marine chlorides (i.e. severe cracking and spalling of the concrete cover) exhibit low seismic resistance to earthquake events; this observation is clear at time of 40 and 50 years where the structure reduces its capacity by 100 % compared to the pristine condition. Yet, the latter is also due to poor concrete quality, seismic details and structural design according to old non-seismic codes. The fragility curves in Figures 5, according to the modified spectral acceleration intensity, confirms the significant impact of the pitting corrosion on RC framed structures. Such effects decrease the seismic vulnerability over time, demonstrating that the multiple excitations are more detrimental than single strong motions. Particularly, the fragility curve at time of 30 years exhibits an increment of the vulnerability equal to 95 % for sequential motions with a mean value of 0.065 m/s, compared to 90 % and 85 % for mainshocks and aftershocks, respectively. Furthermore, the extended plateau in the difference between fragility curves demonstrates how the earthquake sequences force the structure to accumulate more damage than the single motions. As a result, the probability of exceeding the limit state of near collapse at different time is extended for IM values greater than the case study of mainshocks and aftershocks (Figures 4d,4e, 4f, 5d, 5e, 5f).

The outcomes of the comprehensive numerical simulations on the vulnerability investigation of the RC frame through the time-dependent fragility analysis reflects explicitly the capacity degradation and demand increment that the structure would undergo over its service life, but also the need for further studies on the capacity parameters for a better prediction of the seismic vulnerability of such existing RC structures.

6 Conclusions

This paper investigates the time-dependent seismic performance of a typical 4-story RC frame located in aggressive coastal environment in Italy and subjected to single and multiple excitations. The finite element model of the RC frame accounts for the effects of pitting corrosion on the mechanical and geometrical properties of the concrete and the steel reinforcement. Probabilistic approach is herein considered both for the mechanical and geometrical properties of steel and concrete, and the time initiation and propagation of pitting corrosion. Fifteen natural ground motions are collected from international database and a time gap of ten times the first natural periods of the RC frame is employed between the mainshock and aftershocks to simulate seismic sequences. The fragility assessment is conducted through the incremental dynamic analysis for two seismic intensity measure and considering the limit state of near collapse. The following conclusions are drawn by analysis of the obtained results:

The multiple excitations produced larger impacts on the corroded RC frame structure. Both intensity measure, in fact, showed the highest decrease in the seismic vulnerability of such earthquake swarms compared to single ground motions. For instance, the decrease was equal to 65 % at time of 30 years for the seismic sequences in comparison with 60 % for aftershock and mainshock motions

The mean that would cause a failure probability of 50 % decreases over the lifetime of the RC frame, both for single and multiple motions. For example, sequential earthquakes produced a reduction of the mean equal to 95 %, while 90 % and 88 % were recorded for mainshocks and aftershocks, respectively.

Both the flexural and the shear capacity had a significant reduction due to pitting corrosion. The last observation can be found in the decrease of the mechanical parameters of the steel and concrete. As a result, further studies should focus on the capacity formulations to find whether or not they still hold when corrosion occurs.

Acknowledgements

The authors would like to acknowledge the gracious support of this work through the EPSRC and ESRC Centre for Doctoral Training on Quantification and Management of Risk and Uncertainty in Complex Systems Environments Grant No. (EP/L015927/1).

References

[1] Ruiz-García, J. (2012): Mainshock-aftershock ground motion features and their influence in 654 building's seismic response, J. Earthq. Eng., 16(5): 719–737.

[2] Di Sarno, L., Pugliese, F., (2021): Effects of mainshock-aftershock sequences on fragility analysis of RC buildings with ageing, Engineering Structures, Volume 232, 2021, 111837, ISSN 0141-0296, https://doi.org/10.1016/j.engstruct.2020.111837.

[3] Abdelnaby, Adel, E. (2018): Fragility Curves for RC Frames Subjected to Tohoku Mainshock-542 Aftershocks Sequences. Journal of Earthquake Engineering, Volume 22, Pages 902-920, 543 Taylor & Francis, https://doi.org/10.1080/13632469.2016.1264328.

[4] Hosseinpour, F., Abdelnaby, A.E. (2017): Fragility curves for RC frames under multiple earthquakes, Soil Dynamics and Earthquake Engineering, Volume 98, 2017, Pages 222-234, ISSN 0267-7261, https://doi.org/10.1016/j.soildyn.2017.04.013.

[5] Li, Q., Ellingwood, B.R. (2007): Performance evaluation and damage assessment of steel frame buildings under main shock–aftershock earthquake sequences. Earthquake Engineering and Structural Dynamics, Volume 36 Issue 3, Pages 405-42. https://doi.org/10.1002/eqe.667.

[6] Ma, Y., Guo, Z., Wang, L., Zhang, J. (2020): Probabilistic Life Prediction for Reinforced Concrete Structures Subjected to Seasonal Corrosion-Fatigue Damage. Journal of Structural Engineering, ASCE, Volume 146, Issue 7, doi: 10.1061/(ASCE)ST.1943-541X.0002666

[7] Di Sarno, L., Pugliese, F. (2020a): Numerical evaluation of the seismic performance of existing reinforced concrete buildings with corroded smooth rebars. Bull Earthquake Eng 18, 4227–4273 (2020). https://doi.org/10.1007/s10518-020-00854-8

[8] Vamvatsikos, D., Cornell, C.A. (2002): Incremental dynamic analysis. Earthquake Eng. Struct. Dyn., 31: 491-514. doi:10.1002/eqe.141.

[9] Jalayer, F., De Risi, R., Manfredi, G. (2015): Bayesian Cloud Analysis: efficient structural fragility assessment using linear regression. Bull Earthquake Eng 13, 1183–1203. https://doi.org/10.1007/s10518-014-9692-z

[10] Padgett, J.E., Nielson, B.G., Des Roches, R. (2008): Selection of optimal intensity measures in probabilistic seismic demand models of highway bridge portfolios. Earthquake Eng. Struct. Dyn., 37: 711-725. doi:10.1002/eqe.782.

[11] EN 1998-1, 2004. Eurocode 8: Design Of Structures For Earthquake Resistance. 1st ed. 583 Brussels: BSi.

[12] DuraCrete (2000): General guidelines for durability design and redesign. The European Union—Brite EuRam III, Research Project No. BE95-1347. Probabilistic performance-based durability design of concrete structures. Document Report 15:109

[13] Vidal, T., Castel, A., François, R. (2004): Analyzing crack width to predict corrosion in reinforced concrete, Cement and Concrete Research, Volume 34, Issue 1, Pages 165-174, ISSN 0008-8846, https://doi.org/10.1016/S0008-8846(03)00246-1.

[14] Rodriguez, J., Ortega, L.M., Casal, J. (1997): Load carrying capacity of concrete structures with corroded reinforcement. Constr Build Mater 1997; 11(4):239–48.

[15] Torres-Acosta, A.A., Martinez-Madrid, M. (2003): Residual life of corroding reinforced concrete structures in marine environment. J Mater Civ Eng ASCE 2003;15(4):344–53.

[16] Linwen, Yu, Raoul, François, Vu, Hiep, Dang, Valérie, L'Hostis, Richard, Gagné (2015): Distribution of corrosion and pitting factor of steel in corroded RC beams, Construction and Building Materials, Volume 95, 2015, Pages 384-392, ISSN 0950-0618, https://doi.org/10.1016/j.conbuildmat.2015.07.119.

[17] DuraCrete (2000): Statistical Quantification of the Variables in the Limit State Functions. The European Union Brite EuRam 3 contract BRPR-CT95-0132 Project BE95-1347 Report no BE95-1347/R7 May 2000.

[18] Vidal, T., Castel, A., François, R. (2004): Analyzing crack width to predict corrosion in reinforced concrete, Cement and Concrete Research, Volume 34, Issue 1, 2004, Pages 165-174, ISSN 0008-8846, https://doi.org/10.1016/S0008-8846(03)00246-1.

[19] Palle Thoft-Christensen: Stochastic Modeling of the Crack Initiation Time for Reinforced Concrete structures, Advanced Technology in Structural Engineering, DOI: 10.1061/40492(2000)157